

# Robust accidental nodes and zeroes and critical quasiparticle scaling in iron-based multiband superconductors

Valentin Stanev

*Materials Science Division, Argonne National Laboratory, 9700 South Cass Avenue, Argonne, IL 60439*

Boian S. Alexandrov

*Theoretical Division, Los Alamos National Laboratory, Los Alamos, New Mexico 87545*

Predrag Nikolić

*Department of Physics & Astronomy, George Mason University, MS 3F3, Fairfax, VA 22030*

Zlatko Tešanović

*Institute for Quantum Matter and Department of Physics & Astronomy,  
The Johns Hopkins University, Baltimore, MD 21218*

(Dated: October 12, 2018)

We study multigap superconductivity, with strong angular variations of one of the gaps, as appropriate for certain iron-based high-temperature superconductors. We solve the gap equations of this model and find that the nodes or zeroes in the gap function present at  $T_c$  – although purely accidental – typically survive down to  $T = 0$ . Based on this result, we investigate the line of quantum transitions at which gap zeroes first appear. The peculiar "zero-point" critical scaling emanating from this line dominates quasiparticle thermodynamics and transport properties over much of the phase diagram, and supplants more familiar forms of scaling associated with the accidental nodes.

## I. INTRODUCTION

The discovery of iron-based high-temperature superconducting family<sup>1</sup> has altered the landscape of condensed matter research. The underlying physics of ironpnictides and the first high- $T_c$  family – the cuprates – appear to be significantly different. Thus, after two decades of cuprate domination, the superconductivity research faces new major challenges and new important problems.

The progress in our understanding of iron-pnictides has been swift<sup>2,3</sup>, but many important questions remain unanswered. In particular, the form of the order parameter remains uncertain. There is growing consensus that it belongs to the general class of the so-called  $s_{\pm}$ ,  $s'$  or extended  $s$ -wave state<sup>4</sup>, the basic dynamical origin of which can be understood from analytic renormalization group (RG) arguments<sup>5,6</sup>. This superconducting state is generated by the electron-electron interaction, originating in Coulomb repulsion. This mandates a sign change between the gaps on the multiple sheets of the Fermi surface (FS) (interestingly, a similar order parameter appears within the strong coupling approach to pnictides<sup>7</sup>). In 122s – the best studied compounds of this family – the angle resolved photoemission spectroscopy (ARPES)<sup>8–10</sup> detects up to four relatively isotropic gaps, one for each of the two hole and two electron bands of the FS. This is in an apparent contradiction to the penetration depth<sup>11,12</sup>, thermal conductivity<sup>13</sup> and specific heat data<sup>14,15</sup>, which indicate gapless quasiparticle excitations – a natural interpretation is that these are associated with nodes in the gap somewhere along the (multiply-connected) FS. Moreover, Refs. 13 and 15 report such excitations both in the under- and over-doped phases of (Co,Ba)122, but they

apparently disappear at optimal doping. This suggests a significant change in the gap structure as a function of doping. Similar doping evolution of the gap has been reported based on penetration depth measurements<sup>16</sup>.

Such reading of the experiments receives some support from theory. Random phase approximation (RPA)-based calculations<sup>17,18</sup> hint at a multitude of competing nodal and nodeless states and possible transitions among them, tuned by material parameters like pnictogen height or impurity concentration. Furthermore, fluctuation exchange<sup>19</sup> and numerical functional RG (fRG) studies<sup>20–22</sup> also find significant angular variations and possible nodes in one or more of the gaps. A similar possibility was discussed in a model of Ref. 23. In these studies, the nodal structure is typically induced by the strong *orbital anisotropy* of effective interactions *within* the extended  $s$ -wave state. Thus, such nodes are "accidental," in the sense that they are not protected by any symmetry or topological considerations. Consequently, their presence or absence, and location on the FS are all affected by the interactions, temperature, impurity scattering, and the like.

Both the numerical fRG and RPA studies, as well as Ref. 23, have focused on the *linearized* gap equations and the ensuing pairing states at  $T = T_c$ . However, since the gap equations form a complicated non-linear system there is no guarantee that the gap structure will remain unchanged, and that such accidental nodes or zeroes, present at  $T = T_c$ , survive as  $T \rightarrow 0$ .

In this paper we consider a model of a two-band superconductor, which has a uniform gap on one band (hole) and gap with angular variations on the other (electron) band. The second gap takes the form  $\Delta_0 + \Delta' \cos 4\theta$ ,

which obviously allows nodes for  $\Delta' > \Delta_0$ . As stressed above, both nodal and nodeless states belong to the native  $A_{1g}$  representation of the lattice rotation group and the appearance of nodes is a direct consequence of the orbital anisotropy of the effective interactions. This model emulates the physics of iron-pnictides and its different versions have been used in that context<sup>23–26</sup>. A summary of our results is as follows: i) The gap structure obtained at  $T = T_c$  is fairly robust as a function of  $T$  and, in particular, if nodes exist near  $T_c$  they can survive as  $T \rightarrow 0$ ; ii) at the zero-points  $\Delta' = \Delta_0$ , there are gapless quasiparticle excitations with unusual anisotropic dispersion. This leads to a distinctive power-law temperature behavior of many thermodynamic quantities; iii) At  $T = 0$  these zero-points form a surface of quantum phase transitions with novel and peculiar anisotropic scaling. Consequently, the familiar Simon-Lee scaling<sup>27</sup> of Dirac-like nodes is superseded by a different form of scaling – this provides us with a new diagnostic tool to apply to the phenomenology of pnictides.

## II. THE STRUCTURE OF THE GAP FUNCTION

The two-band model reflects the basic features of iron-pnictides: a hole-like and an electron-like band at the center and at the corner of a square Brillouin zone (BZ), respectively. These bands are coupled via interband pairing interaction  $N(0)V(k, k') = \lambda_0 + \lambda_n \cos 4\theta$ , where  $N(0)$  is the density of states (DOS) at the FS,  $\lambda_0$  and  $\lambda_n$  are coupling constants and  $\theta$  is an angle on the electron FS (using coordinate system centered at the electron pocket). Defining gap functions  $\Delta_h(\theta) \equiv \Delta_h$  and  $\Delta_e(\theta) \equiv \Delta_0 + \Delta' \cos 4\theta$  and introducing intraband repulsion  $\mu$  results in the gap equations:

$$\begin{aligned} \Delta_h &= - \int_0^\Lambda d\xi \int_0^{2\pi} \frac{d\theta}{2\pi} \frac{\tanh(E_e/2T)}{E_e} (\lambda_0 + \lambda_n \cos 4\theta) \Delta_e \\ &\quad - \mu \int_0^\Lambda d\xi \frac{\tanh(E_h/2T)}{E_h} \Delta_h \\ \Delta_0 &= - \mu \int_0^\Lambda d\xi \int_0^{2\pi} \frac{d\theta}{2\pi} \frac{\tanh(E_e/2T)}{E_e} \Delta_e \\ &\quad - \lambda_0 \int_0^\Lambda d\xi \frac{\tanh(E_h/2T)}{E_h} \Delta_h \\ \Delta' &= - \lambda_n \int_0^\Lambda d\xi \frac{\tanh(E_h/2T)}{E_h} \Delta_h, \end{aligned} \quad (1)$$

where  $\Lambda$  is a high-energy cut-off and  $E_e \equiv \sqrt{\xi^2 + \Delta_e^2}$ ;  $E_h \equiv \sqrt{\xi^2 + \Delta_h^2}$ . Since all interactions are repulsive  $\langle \Delta_e \rangle_{FS} \Delta_h < 0$  is a necessary condition for non-trivial solutions of Eqs. (1) to exist ( $\langle \dots \rangle_{FS}$  is the angular average over the electron FS). Such sign-switching state is a likely prospect for pnictides<sup>2</sup>. For  $T \rightarrow T_c$ , these equations can be linearized with the following result (see also Ref. 23): when  $\Delta' = \Delta_0$ , there are four zeroes in

$\Delta_e$  at  $(p_F, 0)$ ,  $(0, p_F)$ ,  $(-p_F, 0)$  and  $(0, -p_F)$  (using coordinate system, rotated by  $\pi/4$  with respect to BZ axes, and where  $p_F$  is the Fermi momentum for the electron band). The same structure is reproduced at other corners of the BZ. It is important to stress here that, while (1) is a simplified phenomenological model, the physics and the results that are the focus of this paper will *remain unchanged* when a more realistic description is employed.

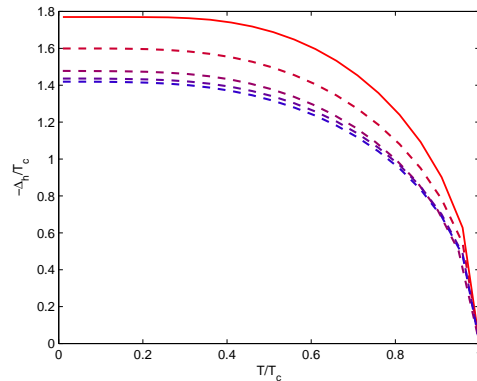


FIG. 1.  $\Delta_h(T)/T_c$  as obtained from solving eqs. (1). The solid red line is for parameter values  $\mu = 0.05$ ;  $\lambda_0 = 0.2$  and  $\lambda_n = 0$ , and corresponds to the BCS result for a single band. Increasing  $\lambda_n = 0$  from zero leads to *decrease* in  $\Delta_h/T_c$  - shown for  $\lambda_n = 0.1$ ,  $\lambda_n = 0.15$ ,  $\lambda_n = 0.2$  and  $\lambda_n = 0.3$  (the blue component increases with increasing  $\lambda_n$ ). Note the negative sign of  $\Delta_h$  - consequence of choosing  $\Delta_0$  positive.

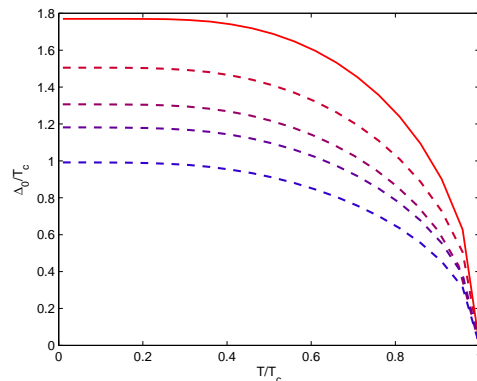


FIG. 2.  $\Delta_0(T)$  obtained from solving eqs. (1). The parameters, color coding and normalization are the same as in Fig. 1.

The first such result follows from solving eqs. (1) at arbitrary  $T$ , a complicated task which we accomplish numerically. Representative results for  $\Delta_h$ ,  $\Delta_0$  and  $\Delta'$  and are displayed in Figs. 1, 2 and 3. For  $\lambda_n = 0$  the model reduces to the case of two uniform gaps which follow (for equivalent bands) the BCS temperature dependence (a known result for multiband superconductors<sup>28,29</sup>). A

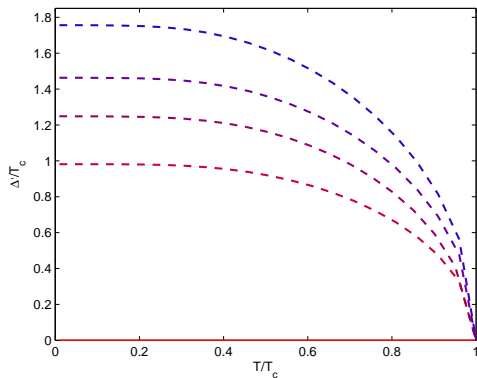


FIG. 3.  $\Delta'$  as function of temperature. The parameters, color coding and normalization are the same as in Fig. 1.

nonzero value of  $\lambda_n$  generates a finite  $\Delta'$ , and pushes  $\Delta_0/T_c$  and  $\Delta'/T_c$  below their BCS values (of course, in absolute units  $T_c, \Delta_0$  and  $\Delta_h$  all go up). Evidently, the temperature dependence of different gaps is *similar*. Most importantly, this implies that  $\Delta'/\Delta_0$  has a rather weak  $T$  dependence and a nodal state at  $T = T_c$  will thus likely remain nodal as  $T$  goes to 0 (shown on Fig. 4). Remarkably,  $\Delta'(T)/\Delta_0(T)$  can both increase or decrease or can even exhibit a non-monotonic behavior, testifying to the strong non-linearity of the gap equation. Nevertheless, the overall changes are generically quite small. Thus, the  $T = T_c$  phase diagram survives at  $T = 0$  without major changes (Fig. 5 shows our phase diagram, with  $\lambda_0$  fixed). We also point out that  $\Delta_0(T \rightarrow 0)/\Delta_h(T \rightarrow 0)$  is not equal to  $\Delta_0(T \rightarrow T_c)/\Delta_h(T \rightarrow T_c)$  as expected for isotropic two-band superconductor<sup>30</sup>.

The above results are surprising since the nodes are only accidental and therefore sensitive to disruption by the strongly non-linear nature of the gap equations (1). Their robustness can be viewed as *a posteriori* justification for the use of nodal or near nodal states in low  $T$  calculations, since previously these states were self-consistently obtained only at  $T_c$ . Note also that the three coupling constants of our model lead to a certain ambiguity: a nodal state can be created by large  $\lambda_n$  or by strong  $\mu$ , since intraband repulsion suppresses the uniform gap stronger than the oscillating one. These two distinct mechanisms of generating nodes – a very anisotropic interband interaction and a strong intraband repulsion – are both present in pnictides, and reflect genuine physics of these multiband superconductors. Furthermore, because the number of gaps in real materials is (at least) four, there is additional frustration associated with interband pair scattering between the gaps with the same sign. This frustration effect also favors the nodal components<sup>22</sup>, and should be included in a more realistic four or five-band calculations.

The second key result follows from the first: consider the surface  $\Delta' = \Delta_0$  in the  $(\lambda_n, \mu, T)$  space (with  $\lambda_0$

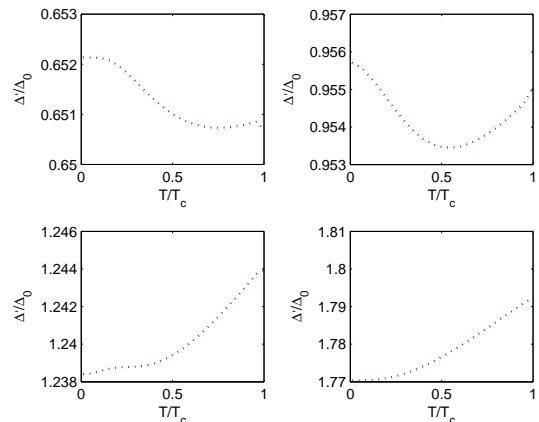


FIG. 4. Ratio  $\Delta'(T)/\Delta_0(T)$ , arising from solution of Eqs. (1) for  $\mu = 0.05$ ;  $\lambda_0 = 0.2$  and  $\lambda_n = 0.1, 0.15, 0.2, 0.3$ , respectively. This ratio does not have a simple temperature behavior, but the changes are generically quite small. This means that the nodes, present at  $T = T_c$ , likely survive as  $T \rightarrow 0$ .

fixed), and ignore  $\Delta_h$  since its contribution is exponentially suppressed at low  $T$ . On this surface the gap in the electron band develops four zeroes, which, for  $\Delta' > \Delta_0$ , split into eight nodes. At  $T = 0$ , this surface defines a *line of quantum phase transitions* (see Fig. 5), along which the low energy quasiparticle spectrum suffers a non-analytic transformation. For  $\Delta' < \Delta_0$ , the quasi-

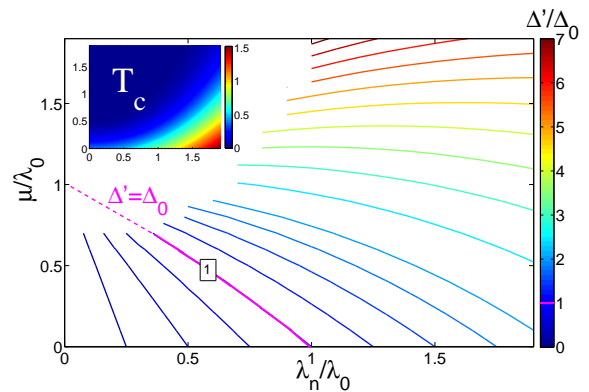


FIG. 5. The  $\Delta'/\Delta_0$  isolines for various  $\mu$  and  $\lambda_n$ , with  $\lambda_0 = 0.2$ . All of them converge at  $\mu = \lambda_0$  point at the  $y$ -axis. The color axis represents  $\Delta'/\Delta_0$ . For numerical convenience  $T$  is kept finite, but extremely small ( $T = 10^{-5}T_c$ ), and is practically zero. Inset: color map of  $T_c$  (in arbitrary units) for the same values of  $\mu$  and  $\lambda_n$ .

particle excitations are gapped whereas, for  $\Delta' > \Delta_0$ , one enters the nodal region, with gapless Bogoliubov-deGennes (BdG) quasiparticles described by a Dirac-like Hamiltonian<sup>27</sup>. At the critical line  $\Delta' = \Delta_0$  separating the two regimes – where the pairs of nodes merge

into zeroes – the quasiparticle dispersion has a peculiar character: linear along the Fermi velocity and quadratic perpendicular to it (see Fig. 6). The resulting spectrum gives rise to an unusual critical scaling of low  $T$  thermodynamics, which dominates the phase diagram surrounding the critical line.

### III. ZEROES IN THE GAP FUNCTION AND THEIR SIGNATURES IN QUASIPARTICLE PHENOMENOLOGY

To explore this peculiar criticality at the  $\Delta' = \Delta_0$  line, we expand the gap function in the BdG Hamiltonian around one of the zeroes, say  $(p_F, 0)$ :

$$\mathcal{H}_{\text{BdG}} = \begin{bmatrix} \frac{\mathbf{p}^2}{2m} - \epsilon_F & \hat{\Delta}(\mathbf{r}) \\ \hat{\Delta}(\mathbf{r}) & -\frac{\mathbf{p}^2}{2m} + \epsilon_F \end{bmatrix} \approx \begin{bmatrix} v_F p_x & \frac{8\Delta_0}{p_F^2} p_y^2 \\ \frac{8\Delta_0}{p_F^2} p_y^2 & -v_F p_x \end{bmatrix} \quad (2)$$

Eq. (2) results in an anisotropic dispersion  $E = \sqrt{(v_F p_x)^2 + (8\Delta_0 p_y^2/p_F^2)^2}$  for quasiparticle energies. This leads to anisotropic scaling and different low-energy ( $E \ll \Delta_0$ ) scaling lengths along  $x$  and  $y$  directions:  $v_F/E$  and  $\sqrt{v_F a/E}$ , respectively, where  $a = (8\Delta_0/v_F p_F^2)$ . In the Lagrangian nomenclature, the scaling dimensions at  $T = 0$  are  $[y] = -1$ ,  $[x] = -z_x$ ,  $[\tau] = -z_\tau$ , where  $z_\tau = z_x = 2^{31}$ .

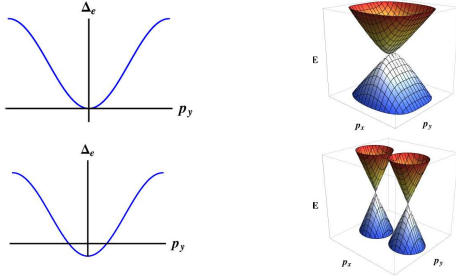


FIG. 6. The quasiparticle dispersion near accidental zeroes and nodes. For strongly anisotropic gap,  $|\Delta_0 - \Delta'| \ll \Delta_0$ , the "zero-point" critical scaling dominates the nodal contribution.

We can now evaluate the DOS of BdG quasiparticles:

$$N_e(E) = \left\langle \text{Re} \left( \frac{E}{\sqrt{E^2 - \Delta(\theta)^2}} \right) \right\rangle_{FS} \sim \sqrt{E} \quad (3)$$

which is different from the familiar nodal DOS  $N_d(E) \sim E$ . This increase of DOS relative to the nodal case is caused by the parabolic part in  $E$ . An exact expression, in terms of complete elliptic integrals<sup>32</sup>, is:

$$N_e(E) = \frac{N_z}{2\pi} \sqrt{\frac{E}{\Delta_0}} K(q), \quad \text{where } q = \sqrt{1 + \frac{E}{2\Delta_0}}; \quad (4)$$

where  $N_z$  is the number of gap zeroes, and as expected, for  $E \rightarrow 0$ ,  $N_e(E) \rightarrow \sqrt{E}$ .

We have calculated the total DOS –  $N_{\text{tot}}(E, T) = N_e(E, T) + N_h(E, T)$  – by using the gap functions shown in Figs. 1, 2 and 3. The results (at  $T = 0$ ) are displayed in Fig. 7. Clearly, the DOS exhibits a complex behavior with several prominent features. First, the two coinciding (at  $\lambda_n = 0$ ) BCS singularities in  $N_e$  and  $N_h$  at  $E = \Delta_h = \Delta_e$ , split for a nonzero  $\lambda_n$ . In addition, a new peak appears in  $N_e$ , due to the introduction of a new energy scale  $\Delta'$ . The positions of the three peaks evolve with increasing  $\lambda_n$ . For  $\Delta' > \Delta_0$ , the low-energy excitations exist all the way down to  $E = 0$ , as expected for nodal order parameter.

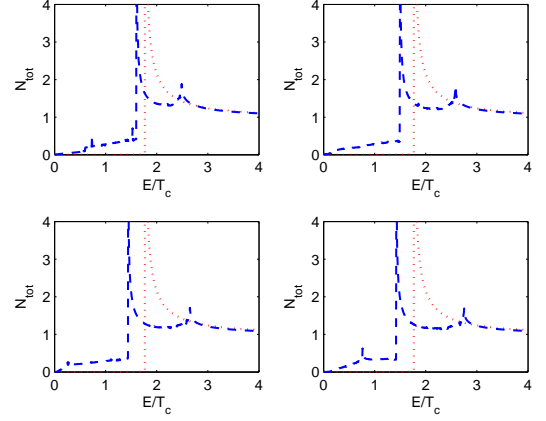


FIG. 7. The total DOS, calculated using the gap functions for  $\lambda_n = 0.1, 0.15, 0.2, 0.3$ , respectively. In each panel the BCS DOS ( $\lambda_n = 0$ ) is included for comparison.

Having determined DOS, we are now in position to extract the low  $T$  dependence of various thermodynamic quantities. The specific heat can be written as:

$$C(T) \approx \frac{N_z}{T^2} \int_0^\infty dE \frac{E^2 N(E)}{\cosh^2(E/2T)} \sim N_z T^{3/2}. \quad (5)$$

Similarly, we can obtain the temperature dependence of the spin susceptibility and the superfluid density:

$$\begin{aligned} \chi_s(T)/\chi_n &= 1 - \rho_s(T)/\rho_0 \approx \\ &\approx \frac{N_z}{2T} \int_0^\infty dE \frac{N(E)}{\cosh^2(E/2T)} \sim N_z T^{1/2}, \end{aligned} \quad (6)$$

from which we can obtain the leading temperature-dependent term of the penetration depth:

$$\lambda(T) = \sqrt{\frac{c^2 m}{4\pi e^2 \rho_s(T)}} \sim \lambda(0) + \lambda_1 T^{1/2}. \quad (7)$$

The nuclear spin relaxation rate is:

$$\frac{(T_1)_n}{(T_1)_s} \approx \frac{N_z}{T} \int_0^\infty dE \frac{N(E)^2}{\cosh^2(E/2T)} \sim N_z T. \quad (8)$$

For the thermal conductivity we need the quasiparticle scattering rate, which can be written as:

$$\frac{1}{\tau_{\mathbf{k}}} = N_z \frac{1}{\tau_n} \frac{N(E)}{N_n} \left( 1 - \frac{\Delta_0 \Delta_{\mathbf{k}}}{E_{\mathbf{k}}^2} \right)$$

where  $\tau_n^{-1}$  and  $N_n$  are the normal state scattering rate and DOS respectively. The thermal conductivity in the superconducting state is:

$$\kappa_{ij} \sim \frac{N_z}{T^2} \int_0^\infty dE \frac{E}{\cosh^2(E/2T)} \frac{1}{N(E)} \times \int d\Omega \hat{k}_i \hat{k}_j \left( 1 - \frac{\Delta_0 \Delta_{\mathbf{k}}}{E_{\mathbf{k}}^2} \right) \sqrt{E^2 - \Delta_{\mathbf{k}}^2},$$

where  $k_i$  is the  $i$ th component of the quasiparticle momentum. Integrating around the zeroes and keeping only the term with the lowest power of the temperature, we get for the thermal conductivity, normalized by the normal state value:

$$\frac{(\kappa_0/T)}{(\kappa_n/T)} \approx \frac{N_z}{T^2} \int_0^\infty \frac{dE E^5/2}{N(E) \cosh^2(E/2T)} \sim N_z T. \quad (9)$$

All of the derived scaling forms strictly apply only at the critical line. Of course, tuning precisely to a point on this line is not an easy task experimentally, and this means that the asymptotic low temperature behavior of the thermodynamic quantities will ultimately be governed either by the nodal Dirac or by thermally excited gapped BdG quasiparticles, depending on which side of the line the system finds itself. Importantly, however, as long as one is in the vicinity of the quantum critical line, this asymptotic behavior will be restricted to a *very narrow* low temperature range,  $T \ll |\Delta_0 - \Delta'|$ , and there will be a *large wedge-shaped crossover regime*, dominated by the quantum phase transition, for which the temperature scalings are governed by Eqs. (5)–(9).

We supply an illustration of the above ideas by calculating the spin susceptibility as  $\Delta' \rightarrow \Delta_0$ , and the result is shown in Fig. 8. The low-temperature part of  $\chi_s(T)$  is clearly enhanced, and close to  $\Delta' = \Delta_0$  (for  $\lambda_n = 0.15$ ) the  $T^{1/2}$  crossover behavior is expected.

#### IV. GAP ZEROES IN FINITE MAGNETIC FIELD

Next, we turn to the problem of a superconductor with gap zeroes in an external magnetic field  $H$ . Finite  $H$  modifies the critical line in the  $(\lambda_n, \mu)$  plane, but, for  $H$  far below the upper critical field  $H_{c2}(0)$ , such modifications are negligible. The presence of gapless fermions makes the finite  $H$  problem rather nontrivial, due to the singular scattering of fermions from vortices<sup>33</sup>. Useful results, however, can be extracted from general scaling arguments; in nodal  $d$ -wave superconductors such arguments are behind the well-known Simon-Lee scaling<sup>27</sup>.

We concentrate on intermediate fields ( $H_{c1} \ll H \ll H_{c2}$ ), where the vortex spacing is large and we can

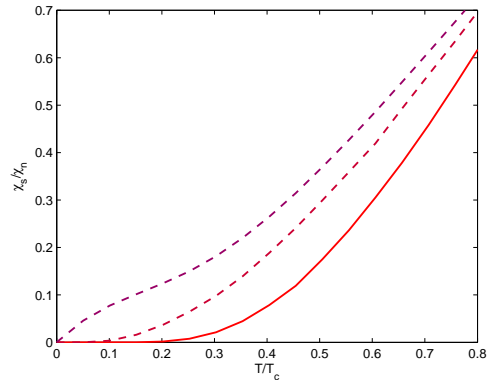


FIG. 8. The spin susceptibility, calculated using the temperature dependence of the gap functions for  $\lambda_n = 0, 0.1$ , and  $0.15$ . The enhancement of the low-temperature part is clearly visible. The case  $\lambda_n = 0.15$  lies almost on the critical line and thus  $\chi_s(T) \sim T^{1/2}$  is expected as a crossover behavior at low temperatures.

assume a uniform field and a constant gap amplitude. Near the  $(p_F, 0)$  zero, the continuum limit of the gauge-invariant gap function takes the form  $\hat{\Delta}(\mathbf{r}) = (8/p_F^2) \{ \partial_y, \{ \partial_y, \Delta(\mathbf{r}) \} \} + (2i/p_F^2) \Delta(\mathbf{r}) \partial_y^2 \phi$ , where  $\Delta(\mathbf{r}) = |\Delta| e^{i\phi(\mathbf{r})}$  and  $\{, \}$  signifies full symmetrization<sup>33</sup>. This allows us to write the low-energy BdG Hamiltonian as:

$$\mathcal{H}_{\text{BdG}} = \begin{bmatrix} \frac{1}{2m} (\hat{\mathbf{p}} + \frac{e}{c} \mathbf{A})^2 - \epsilon_F & \hat{\Delta}(\mathbf{r}) \\ \hat{\Delta}^*(\mathbf{r}) & -\frac{1}{2m} (\hat{\mathbf{p}} - \frac{e}{c} \mathbf{A})^2 + \epsilon_F \end{bmatrix} \approx \begin{bmatrix} v_F(p_x + \frac{e}{c} A_x) & \hat{\Delta}(\mathbf{r}) \\ \hat{\Delta}^*(\mathbf{r}) & -v_F(p_x - \frac{e}{c} A_x) \end{bmatrix}. \quad (10)$$

We now choose Landau gauge  $A_x = Hy$  and rewrite  $v_F(p_x + (e/c)Hy)$  in dimensionless form by introducing a length  $d$  and defining variables  $x' = x/d$  and  $y' = yd/l^2$ , where  $l = \sqrt{c/eH}$  is the magnetic length. The off-diagonal terms in  $\mathcal{H}_{\text{BdG}}$  are similarly rewritten as  $(8\Delta_0/p_F^2) \{ \partial_{y'}, \{ \partial_{y'}, e^{i\phi} \} \} + (i/4) e^{i\phi} (\partial_{y'}^2 \phi) = (v_F a d^2 / l^4) \{ \partial_{y'}, \{ \partial_{y'}, e^{i\phi} \} \} + (i/4) e^{i\phi} (\partial_{y'}^2 \phi)$  and its complex conjugate. The choice  $d = (l^4/a)^{1/3}$  allows us to reexpress the quasiparticle energy spectrum as  $\{E_n\} \rightarrow (v_F/d) \{\varepsilon_n\} = v_F (a/l^4)^{1/3} \{\varepsilon_n\} = v_F (ae^2 H^2 / c^2)^{1/3} \{\varepsilon_n\}$ , where  $\{\varepsilon_n\}$  are numbers which in principle can depend only on  $H/(c/ea^2) \equiv H/H_a \ll 1$ . If they do, such “anomalous” scaling would not be surprising in our case of singular anisotropy. Adding the contributions from all zeroes restores the  $x \leftrightarrow y$  symmetry.

Using the above rescaling, we write DOS  $N(E, H)$  as:

$$\sim \sqrt{v_F} (ae^2 H^2 / c^2)^{1/6} \mathcal{N} \left( \frac{E}{v_F (ae^2 H^2 / c^2)^{1/3}}; \frac{H}{H_a} \right) \quad (11)$$

where  $\mathcal{N}(u; w)$  is the scaling function. If  $H$  induces finite DOS at low  $E$ , we can follow earlier discussion to

obtain  $N(E \rightarrow 0, H) \sim H^{1/3+\eta}$ , where  $\eta > -1/3$  is the "anomalous" dimension, defined by  $\mathcal{N}(u = 0; w \rightarrow 0) = \text{const.} \times w^\eta$ .  $\eta \neq 0$  is clearly a possibility given the fact that the vortex lattice structure in  $\exp(i\phi(\mathbf{r}))$  is determined by *all* electrons and does not conform to the anomalous scaling of individual zero-points. The precise value of  $\eta$  follows from direct computation<sup>34</sup>.

The critical "zero-point" scaling also works when both  $H$  and  $T$  are finite. The internal energy density can be written as

$$U(H, T) = \frac{N_z}{V} \sum_n E_n(H) f(E_n(H)/T) \sim \quad (12)$$

$$\sim N_z H^{5/3} \mathcal{F}_u(T/(v_F^3 a e^2 c^{-2} H^2)^{1/3}; H/H_a),$$

where  $f$  is the Fermi function and  $\mathcal{F}_u$  is a scaling function. Here we converted  $\sum_n \rightarrow (V/4\pi^2) \int dp_x dp_y, dp_x dp_y \sim (1/l^2) dp_x dp_y$ <sup>33</sup>. From (13), the specific heat per unit volume is:

$$C(H, T) \sim N_z H^{5/3} \partial_T \mathcal{F}_u(T/(v_F^3 a e^2 c^{-2} H^2)^{1/3}; H/H_a) \sim$$

$$\sim N_z H \mathcal{F}_c(T/(v_F^3 a e^2 c^{-2} H^2)^{1/3}; H/H_a), \quad (13)$$

where  $\mathcal{F}_c(T/(v_F^3 a e^2 c^{-2} H^2)^{1/3}; H/H_a)$  is the corresponding scaling function.

In general, evaluating  $\mathcal{F}_u$  or  $\mathcal{F}_c$  is a difficult task. However, the needed limits of these functions are readily deduced: Eq. (5) mandates  $\mathcal{F}_c(\alpha \rightarrow \infty; w \rightarrow 0) \rightarrow \alpha^{3/2}$ , where  $\alpha = T/(v_F^3 a e^2 c^{-2} H^2)^{1/3}$ . In the opposite case,  $\alpha \rightarrow 0$ , we can use the constant low  $E$  DOS, induced by  $H$ , and observe that (5) gives  $C(H, T) \sim TH^{1/3+\eta}$ , and thus  $\mathcal{F}_c(\alpha \rightarrow 0; w \ll 1) \rightarrow \alpha w^\eta$ . Note that these scaling arguments apply only to the critical BdG fermions inhabiting the zeroes. We are not including the contributions from other parts of the system, like possible localized states in the vortex cores – this contribution is subleading at low  $E, T$  and  $H$ .

Again, we want to emphasize that although precise tuning to a state with gap zeroes seems very unlikely,

close to such state and at not too small  $T$  and  $H$  the scaling associated with gap zeroes dominates. Thus, in a state with accidental nodes the Simon-Lee scaling can be completely unobservable.

## V. CONCLUSIONS

In summary, we have studied an anisotropic two-band model of iron-based superconductors. By explicit solution of the gap equations, we uncovered the robust nature of the accidental nodes and zeroes in the gap function. We have discussed in some detail the quantum critical line where the gap zeroes first appear. It projects a considerable influence over the phase diagram and is characterized by a peculiar form of anisotropic critical scaling, qualitatively distinct from the familiar Dirac-Simon-Lee scaling. Irrespective of whether one can tune in precisely to this quantum critical line in a particular experiment, as long as the gap is strongly anisotropic ( $|\Delta_0 - \Delta'| \ll \Delta_0$ ), the "zero-point" critical scaling will dominate the quasiparticle thermodynamics and transport over a wide region in a phase diagram, overwhelming the contribution from accidental nodes.

## VI. ACKNOWLEDGMENTS

Work at the Johns Hopkins-Princeton Institute for Quantum Matter were supported by the U. S. Department of Energy, Office of Basic Energy Sciences, Division of Materials Sciences and Engineering, under Award No. DE-FG02-08ER46544. Research at Los Alamos National Laboratory is carried out under the auspices of the U.S. Department of Energy under Contract No. DE-AC52-06NA25396. P.N. is supported by the Office of Naval Research grant N00014-09-1-1025A.

<sup>1</sup> Y. Kamihara, T. Watanabe, M. Hirano, and H. Hosono, J. Am. Chem. Soc. **130**, 3296 (2008).

<sup>2</sup> P. C. W. Chu *et al.* (eds.), *Superconductivity in iron-pnictides*. Physica C **469** (special issue), 313-674 (2009).

<sup>3</sup> J.-P. Paglione and R. L. Green, Nature Phys. **6**, 645 (2010).

<sup>4</sup> I. I. Mazin, D. J. Singh, M. D. Johannes, and M. H. Du, Phys. Rev. Lett. **101**, 057003 (2008).

<sup>5</sup> A.V. Chubukov, D. Efremov, and I. Eremin, Phys. Rev. B, **78**, 134512 (2008).

<sup>6</sup> V. Cvetković and Z. Tešanović, Phys. Rev. B **80**, 024512 (2009).

<sup>7</sup> K. Seo, B. A. Bernevig, and J. Hu, Phys. Rev. Lett. **101**, 206404 (2008).

<sup>8</sup> L. Wray, D. Qian, D. Hsieh, Y. Xia, L. Li, J. G. Checkelsky, A. Pasupathy, K. K. Gomes, C. V. Parker, A. V. Fedorov, G. F. Chen, J. L. Luo, A. Yazdani, N. P. Ong, N. L. Wang, and M. Z. Hasan, Phys. Rev. B **78**, 184508 (2008).

<sup>9</sup> K. Nakayama, T. Sato, P. Richard, Y.-M. Xu, Y. Sekiba, S. Souma, G. F. Chen, J. L. Luo, N. L. Wang, H. Ding, and T. Takahashi, Europhys. Lett. **85**, 67002 (2009).

<sup>10</sup> Y. Zhang, L. X. Yang, F. Chen, B. Zhou, X. F. Wang, X. H. Chen, M. Arita, K. Shimada, H. Namatame, M. Taniguchi, J. P. Hu, B. P. Xie, and D. L. Feng, Phys. Rev. Lett. **105**, 117003 (2010).

<sup>11</sup> C. Martin, H. Kim, R. T. Gordon, N. Ni, V. G. Kogan, S. L. Bud'ko, P. C. Canfield, M. A. Tanatar, and R. Prozorov, Phys. Rev. B **81**, 060505(R) (2010).

<sup>12</sup> K. Hashimoto, M. Yamashita, S. Kasahara, Y. Senshu, N. Nakata, S. Tonegawa, K. Ikeda, A. Serafin, A. Carrington, T. Terashima, H. Ikeda, T. Shibauchi, and Y. Matsuda, arXiv:0907.4399.

<sup>13</sup> J.-Ph. Reid, M. A. Tanatar, X. G. Luo, H. Shakeripour, N. Doiron-Leyraud, N. Ni, S. L. Bud'ko, P. C. Canfield, R. Prozorov, and L. Taillefer, Phys. Rev. B **82**, 064501

- (2010).
- <sup>14</sup> K. Gofryk, A. S. Sefat, M. A. McGuire, B. C. Sales, D. Mandrus, J. D. Thompson, E. D. Bauer, and F. Ronning, *Phys. Rev. B* **81**, 184518 (2010).
  - <sup>15</sup> K. Gofryk, A. B. Vorontsov, I. Vekhter, A. S. Sefat, T. Imai, E. D. Bauer, J. D. Thompson, and F. Ronning, arXiv:1009.1091.
  - <sup>16</sup> R. T. Gordon, H. Kim, N. Salovich, R. W. Giannetta, R. M. Fernandes, V. G. Kogan, T. Prozorov, S. L. Bud'ko, P. C. Canfield, M. A. Tanatar, R. Prozorov, *Phys. Rev. B* **82**, 054507 (2010).
  - <sup>17</sup> K. Kuroki, S. Onari, R. Arita, H. Usui, Y. Tanaka, H. Kontani, and H. Aoki, *Phys. Rev. Lett.* **101**, 087004 (2008).
  - <sup>18</sup> S. Graser, T. A. Maier, P. J. Hirschfeld, and D. J. Scalapino, *New J. Phys.* **11**, 025016 (2009).
  - <sup>19</sup> R. Sknepnek, G. Samolyuk, Y.-B. Lee, and J. Schmalian, *Phys. Rev. B* **79**, 054511 (2009).
  - <sup>20</sup> R. Thomale, C. Platt, J. Hu, C. Honerkamp, and B. A. Bernevig, *Phys. Rev. B* **80**, 180505(R) (2009).
  - <sup>21</sup> Fa Wang, H. Zhai, Y. Ran, A. Vishwanath, and Dung-Hai Lee, *Phys. Rev. Lett.* **102**, 047005 (2009).
  - <sup>22</sup> C. Platt, R. Thomale, and W. Hanke, arXiv:1012.1763.
  - <sup>23</sup> A.V. Chubukov, M.G. Vavilov, and A.B. Vorontsov, *Phys. Rev. B* **80**, 140515(R) (2009).
  - <sup>24</sup> G. R. Boyd, T. P. Devereaux, P. J. Hirschfeld, V. Mishra, and D. J. Scalapino, *Phys. Rev. B* **79**, 174521 (2009)
  - <sup>25</sup> T. Fischer, A. V. Pronin, J. Wosnitza, K. Iida, F. Kurth, S. Haindl, L. Schultz, B. Holzapfel, and E. Schachinger, arXiv:1005.0692.
  - <sup>26</sup> Dong-Jin Jang, A. B. Vorontsov, I. Vekhter, K. Gofryk, Z. Yang, S. Ju, J. B. Hong, J. H. Han, Y. S. Kwon, F. Ronning, J. D. Thompson, and Tuson Park, arXiv:1011.4808.
  - <sup>27</sup> S. H. Simon and P. A. Lee, *Phys. Rev. Lett.* **78**, 1548 (1997).
  - <sup>28</sup> H. Suhl, B. T. Matthias, and L. R. Walker, *Phys. Rev. Lett.* **3**, 552 (1959).
  - <sup>29</sup> V.A. Moskalenko, *Fiz. Met. Metalloved.* **8**, 503 (1959) [*Phys. Met. Metallogr.* **8**, 25 (1959)].
  - <sup>30</sup> V. Z. Kresin, *Jour. Low. Temp. Phys.*, **11**, 519 (1973).
  - <sup>31</sup> S. Sachdev, "Quantum Phase Transitions", Cambridge University Press, (1999).
  - <sup>32</sup> M. T. Béal-Monod and K. Maki, *Phys. Rev. B* **53**, 5775 (1996).
  - <sup>33</sup> M. Franz and Z. Tešanović, *Phys. Rev. Lett.* **84**, 554 (2000); O. Vafek, A. Melikyan, M. Franz, and Z. Tešanović, *Phys. Rev. B* **63**, 134509 (2001).
  - <sup>34</sup> As  $H \rightarrow 0$ , the vortex lattice aspect ratio in the  $(x', y')$ -plane either vanishes or diverges: V. Stanev *et al.*, unpublished. Note that  $\eta = 1/6$  for particle-in-a-box  $l \times l$  with the same anomalous scaling, while the Volovik approximation (G. E. Volovik, *Pis'ma Zh. Eksp. Teor. Fiz.* **58**, 457 (1993) [*JETP Lett.* **58**, 469 (1993)]) gives  $\eta = -1/12$ .